

論文 Simulations of the Localized Failure of RC Shear Walls by FEM

Guo-xiong YU^{*1} and Tada-aki TANABE^{*2}

ABSTRACT: The shear band localization phenomenon can often be observed in RC shear wall structures. The authors have suggested that this phenomenon is caused by the material instability when the material acoustic tensor ceases to be positive [1]. In this paper, it will be shown that how the RC specimen is made when the localization phenomenon is likely to occur. Also, finite element method will be used to simulate this phenomenon and the analytical results will be compared with those of experiments. The specimens analyzed will include two specimens done in Yamanashi university and one big scale RC shear wall carried out by NUEPIC (Nuclear Power Engineering Corporation).

KEY WORDS: RC shear wall experiment, localization phenomenon, acoustic tensor, nonlinear FEM analysis,

1. INTRODUCTION

Experiments showed that the localized shear band can often be seen in RC shear wall structures. For these structures, concrete cracks occur firstly at the early stage of load, however as the external load increases to a certain extent, for some specimen satisfying certain conditions, a shear band will occur within a short interval of time along the direction which is entirely different from the initially formed crack angle. Frequent occurrence of this localized failure mode and its specific appearance have let the authors suggest that this phenomenon is caused by the composed material instability when the composed material acoustic tensor ceases to be positive due to the compressive deterioration in concrete.

In the first part of this paper, a brief review of the finite element method with modified displacement field, which was used in this analysis, will be given. And then, experiments of RC panels will be scrutinized to see under what condition the localized failure phenomenon will occur in the specimen. And finally, the analytical results of RC shear wall structures will be shown. This will include two specimens done in Yamanashi university and one big scale RC shear wall carried out by NUEPIC.

2. SHEAR BAND LOCALIZATION CONDITION

One reason for the localization phenomenon is that the acoustic tensor ceases to be positive definite. In observations, when this kind of localization occurs, large strains can accumulate inside the band, generally called as the shear band, and lead the structures to fracture. The physical mechanism for this phenomenon is that the strain field across the shear band can possibly take a jump, while the equilibrium of the stress across the shear band remains to be satisfied.

The shear band localization condition can be expressed as [2]

$$\det(A(n)) = 0 \quad (1)$$

where $A_{jk}(n) = n_i D_{ijkl} n_l$ is the acoustic tensor and D_{ijkl} is the tangential constitutive matrix of the material.

*1 Research Associate, Dept. of Civil Engineering, Nagoya University, Japan.

*2 Professor, Dept. of Civil Engineering, Nagoya University, Japan.

Eq.(1) can be rewritten as

$$A_{jk}(n)m_k = (n_i D_{ijkl} n_l) m_k = 0 \quad (2)$$

If the material satisfies Eq.(1), then increments of strains can have a jump along the discontinuous surface (Fig.1) as shown by Eq.(3)

$$\|\Delta \varepsilon\| = \Delta \varepsilon^+ - \Delta \varepsilon^- = \alpha \hat{T} = \alpha (m_1 n_1, m_2 n_2, m_1 n_2 + m_2 n_1)^T \quad (3)$$

where α is the strength of the jump mode \hat{T} , while the equilibrium across the discontinuous planes remains to be satisfied. In the local coordinate system $x_1 - y_1$, that is

$$\|\Delta \sigma\| = (\Delta \sigma_{x_1}, \Delta \sigma_{y_1}, \Delta \tau_{x_1 y_1})^T = (0, \Delta \sigma_{y_1}, 0)^T \quad (4)$$

Note that in this paper, tangential constitutive matrix for the composite material composed of concrete and reinforcement mesh was used in Eq.(1) in this analysis.

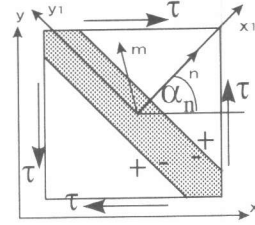


Fig.1 Element with Localization

3. FINITE ELEMENT WITH EMBEDDED LOCALIZED ZONE

In this paper, the shear band localized phenomenon of RC shear wall structures is simulated by finite element with embedded localized zone proposed by Belytschko, et al [2]. In the absence of localization, the strain increments are defined by $\Delta \varepsilon = B \Delta d$, where Δd is the increments of nodal displacement. Once localization occurs, B matrix is assumed as

$$\bar{B} = \begin{cases} \bar{B}_L = (I + \alpha_p (h/b - 1) T T^t) B & \text{in localized zone} \\ \bar{B}_N = (I - \alpha_p T T^t) B & \text{in nonlocalized zone} \end{cases} \quad (5)$$

where $T = \hat{T} / |\hat{T}|$, and the strength of the jump mode $\alpha = \alpha_p (h/b) T^t B \Delta d$, h is the square root of the total area of the element, and b is the shear band width. α_p can be evaluated using Eq.(4). For the sake of the limit of this paper, details to determine \mathbf{n} , \mathbf{m} and α_p which are little bit complicated and can be found in reference [2], will not be given in this paper.

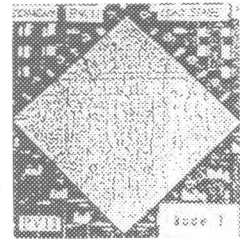
4. EXPERIMENTAL OBSERVATIONS OF THE FAILURE MODES OF RC PANELS

Some experiments have been carried out in the studying of the behavior of RC panels. These include the one by Vecchio and Collins [3]. In this section, through scrutinizing the failure modes of these specimens, we will find out under what condition the localization phenomenon will occur.

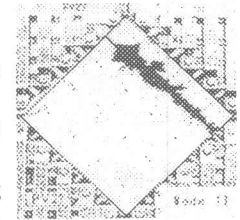
According to the experimental reports, the ultimate failures of the tested panels often involved one of the following three distinguished modes:

1. Yielding of either the longitudinal or transverse steel (Mode I, Fig.2(a)).
2. Sliding shear failure of the concrete prior to yielding of either the longitudinal or transverse steel (Mode II, Fig.2(b)).
3. Preliminary pull out failure due to the imperfection or the stress concentration on the edge of the specimen.

For mode I, the ultimate failure occurred with the initial crack becoming wider and wider and finally the panel failed with the yielding of the reinforcement, but the damage seemed not so localized. But for mode II, the ultimate failure occurred with a shear band formed in the direction entirely different from the initial crack direction, it formed almost parallel to one of the edge of the specimen.



(a) Mode I



(b) Mode II

Fig.2 Failure modes

Table 1: The Angle of the Localization Vector α_n by analysis

Specimen	PV10	PV11	PV22	PV23	PV24	PV27
α_n (analysis)	*	*	85.47°	83.30°	89.03°	90.00°

* means no localization has been detected.

The authors have suggested that the only reason for the specimen failed in mode II with shear band damage, is that it was caused by the material instability when the acoustic tensor ceases to be positive. To prove this analytically, calculations have been carried out on constitutive level in which the increment of the strain was calculated according to the stress increment and the tangential constitutive matrix. The Nagoya University model[4] for RC shear wall, which was formulated through considering the bonding characteristic between concrete and reinforcement, has been used.

In Vecchio and Collins' experiment, there were 26 specimens which had been tested under two-dimensional stress states. There were 6 specimens which had the failure mode II (PV9, PV22, PV27, PV23, PV24, PV25), and 15 specimens which had the failure mode I, the other specimens failed prematurely due to "pull-out" of the shear keys.

The typical shear stress and strain relations, obtained both by analysis and experiment, are shown in Fig.3 for both mode I and mode II by specimen PV11 and PV27, respectively. The point at which the localization occurred is pointed by marking as "▲". Analytical results of the angle between the vector \mathbf{n} and the x axis, α_n (Fig.1), is shown on Tab.1. By experimental observation, α_n is about 90°. After analyzing and examining the experiments, it can be concluded that the mode I was caused by the yielding of the reinforcement when the specimen was so made that at least one of the reinforcement ratio was small or the reinforcement strength was relatively low. On the other hand, when the reinforcement ratio or the reinforcement strength was relatively high or the concrete strength was relatively low, the mode II would possibly occur. Furthermore, when the specimen was subjected to the combined stress state of compression and shear, the mode II was also possibly triggered. Also, the localization occurred at some distance after the peak point where the compressive deterioration of the cracked concrete began.

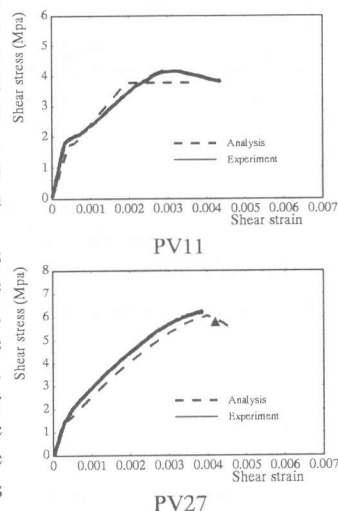


Fig.3 Shear stress and shear strain curves for RC panels

5. FINITE ELEMENT SIMULATIONS OF THE RC SHEAR WALLS

5.1 EXPERIMENT BY YAMANASHI UNIVERSITY

Although up to now, many RC shear wall experiments have been done, as the problem of the localized failure of the shear wall has been ignored, it is necessary to carry out some experiments focusing on this problems. Since the experiment in Yamanashi University is in its early stage, in this paper, the experiment will not be introduced systematically. Here, two specimens with anticipated failure mode I and II, respectively, will be selected, and the finite element which introduced in section 3 is used to see if these two failure modes can be simulated numerically. Briefly, the experimental instrument is shown in Fig.4, external forces can be applied on two sides of the big steel gird above the specimen cyclically, and upon the big steel gird vertically. Steel truss is built to connect this steel gird with the basement in this way that the steel gird can be kept parallel to the basement during the experiment.

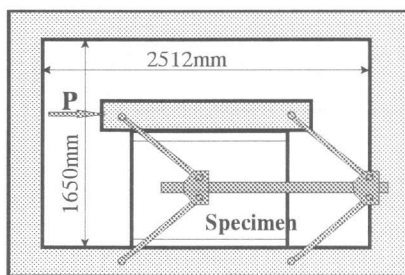


Fig.4 Experiment instrument

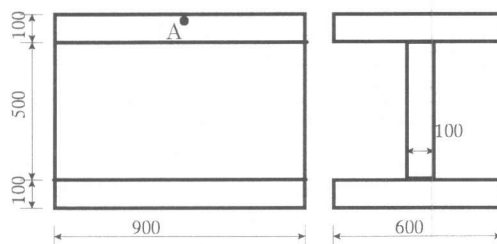


Fig.5 Dimension of specimen 1 (in mm)

(1) The specimen 1 with failure mode I

The dimension of the specimen 1 is shown in Fig.5. The

properties of the material were as follows: $f_c = 358kg/cm^2$,

$f_t = 31.3kg/cm^2$, for horizontal reinforcement

$f_y = 3550kg/cm^2$, and for vertical reinforcement

$f_y = 3819kg/cm^2$. The ratios of reinforcement were rather small,

$\rho_x = 0.6\%$ and $\rho_y = 0.26\%$. Cyclic external force was applied horizontally, and no vertical external was applied.

The analysis was carried out monotonically. Analytically, displacement control at point A (Fig.5) was used in order to obtain the post peak behavior of the specimen. The relation between displacement controlled and the reaction force at the same point is shown in Fig.6 together with that obtained experimentally. Through numerical analysis, it was found that there were no part of the specimen where the concrete underwent compressive deterioration for the compressive stress was small. So, no localization has been detected at any element. For the sake of the special structure of this experiment instrument, at last stage of loading, the specimen seemed to be lifted up from the basement with the reinforcement yielded at the lower part both in the left side and the right side. By Fig.7, this can be proven from the deformed mesh at step marked as "▲" (Fig.6) where ε_y is large in the lower part of specimen, and from the crack pattern (Fig.7) experimentally obtained where a large continuous crack existed in the lower part of the specimen. Just as stated in section 2, as this specimen had strong concrete and was less reinforced relatively, it was not expected to behave in failure mode II at the last stage of loading.

(2) Specimen 2 with failure mode II

Specimen 2 was so made that it was expected to fail in mode II. The dimension of the specimen is shown in Fig.8. The properties of the material were as follows: $f_c = 178kg/cm^2$, $f_t = 17.2kg/cm^2$, $f_y = 3550kg/cm^2$ and $\rho_x = \rho_y = 1.2\%$. The same experiment instrument was used to apply cyclic load horizontally, and vertical load of $30kg/cm^2$ initially.

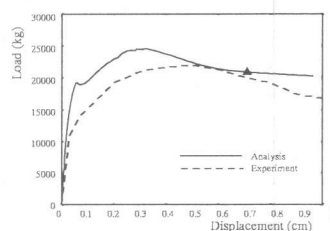


Fig.6 Displacement-load curve for specimen 1

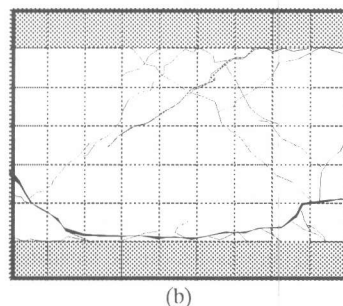
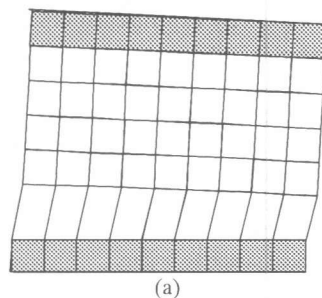


Fig.7

(a) Deformed mesh for specimen 1 at step ▲ by analysis

(b) Crack pattern by experiment

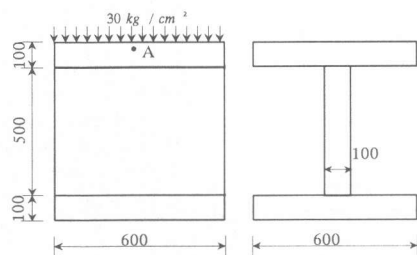


Fig.8 Dimension of specimen 2 (in mm)

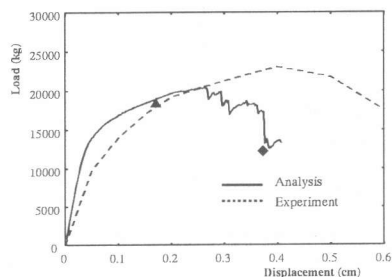


Fig.9 Displacement-load curve for specimen 2

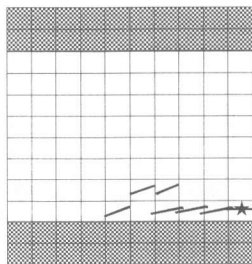


Fig.10 The elements where the localization occurred

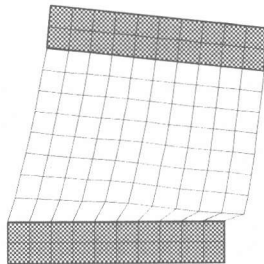


Fig.11 Deformed mesh for specimen 2 at step ◆

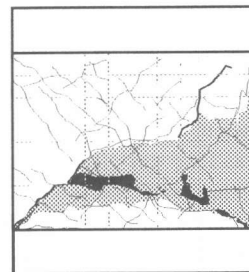


Fig.12 Failure for specimen 2 by experiment

Figure 9 shows the relationship of the force and the displacement at the point controlled (point A in Fig.8). As shown by Fig.9, at step “▲”, the shear band localization firstly occurred at the element “★”(Fig.10). After adding the localization deformation modes to it, the response of the structure was forced to the bifurcation path. It is clear that, for the element with embedded localization modes, less stress is needed than that for the general element to produce the same strain. So, when the localization occurred in the element “★”, the stresses would decrease in this element. Consequently, the stresses of the element on its left side would increase. As a result, the shear localization band would form from element “★” to its left side. Figure 10 shows the elements in which the localization has been detected. Figure 11 shows the deformed mesh at step “◆” in which it can be seen that large strain concentrated into the shear band on the last stage of loading. Figure 12 depicts the failure of the specimen on the last stage, the light shadow shows the region in which the concrete underwent compressive deterioration, and the dark shadow shows the places where the concrete fell down. From Fig.12, it can be seen that the severest failure portion was not on the bottom of the web. Perhaps, this can be explained by the reason that the confinement to the concrete was stronger on the bottom portion.

5.2 EXPERIMENT BY NUPEC

When the RC shear wall structures fail in mode II, the localization shear band does not always form at the bottom of the structure analytically. Some experiments showed it formed at lower part but some distance from the basement as the experiment carried out by NUPEC in which the specimen had strong flanges at the two sides of the web wall.

Figure 13 shows the dimension of the specimen. The properties of the material were as follows:

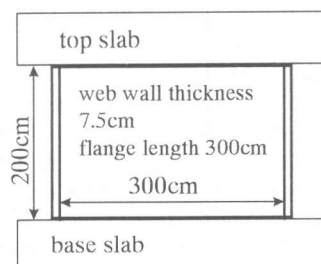


Fig.13 Dimension of specimen by NUPEC

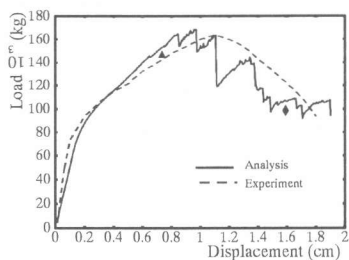


Fig.14 Displacement-load curve for specimen by NUEPEC

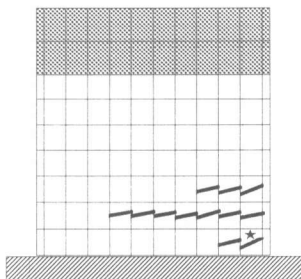


Fig.15 The elements where the localization occurred

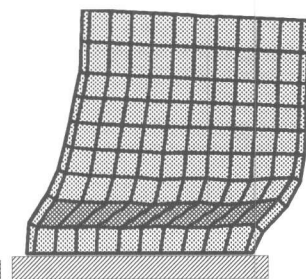


Fig.16 Deformed mesh for at step "◆"

$f_c = 292 \text{ kg/cm}^2$, $f_t = 22.0 \text{ kg/cm}^2$, $f_y = 3910 \text{ kg/cm}^2$ and for the web wall $\rho_x = \rho_y = 1.2\%$. Additional weight was put on the top of the specimen to the extent that the initial resulted compressive stress in the wall was 15 kg/cm^2 . The specimen was excited in horizontal direction by the shaking table.

In this analysis, the effective length of the flanges was taken to be 1/6 of the actual length. Fig.14 shows the analytical and experimental load-displacement results at the top, respectively. At step "▲", the concrete in element "★" underwent compressive deterioration, and the shear band began to form. The elements in which the localization has been detected are shown in Fig.15. Figure 16 shows the deformed mesh at step "◆" with comparison to Fig.17, which shows the eventual failure of the specimen observed experimentally.

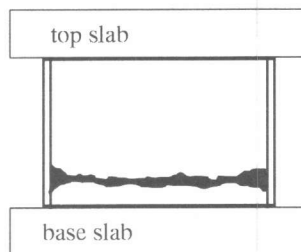


Fig.17 Ultimate failure of the Specimen by experiment

6. CONCLUSION

In this paper, the localization phenomenon has been examined in detail. Mechanically, this phenomenon has been explained as the result of shear band localization when acoustic tensor of the material loss its positive definiteness. When the reinforcement ratio or the reinforcement strength is relatively high, or the concrete strength was low, or the material is under the combined stress state of compression and shear, this phenomenon is likely to occur. Also, in this paper, the finite element with embedded localization zone has been used to successfully simulate this phenomenon in RC shear wall tests. This analytical results are quit in agreement with these of experiments. This can help us to have a thoroughly understanding of the failure mechanism of RC shear walls.

ACKNOWLEDGMENT

The authors thank Nuclear Power Engineering Corporation for their permission of letting their valuable experimental data be used in this paper.

REFERENCES

- [1] Yu,G. and Tanabe, T., "The Analysis of Localized Failure of Reinforced Concrete Shear Wall," Proceedings of JCI, Vol.17, No.2, 1995, pp.1257-1262.
- [2] Belytschdo, T. et al., "A Finite Element with Embeddd Localization Zones," Computer Methods in Applied Mechanics and Engineering, Vol.70, 1989, pp.59-89.
- [3] Vecchio, F.J. and Collins, M.P., "The Respones of Reinforced Concrete to In-plane Shear and Normal Stresses," University of Toronto Publication, No.82-03, March, 1986.
- [4] Wu, Z., Yoshikawa, H. and Tanabe, T., "Tension Stiffness Model for Cracked Reinforced Concrete," ASCE, J. of Struct. Engrg., Vol.117, No.3, 1991, pp.105-114.